Journal of Environmental Science International
35(2); 91~107; February 2026

pISSN: 1225-4517 eISSN: 2287-3503
https://doi.org/10.5322/JESI.2026.35.2.91

ORIGINAL ARTICLE

Spatiotemporal Variation of Particulate Matter ($PM_{2.5}$) Concentration and Hierarchical Clustering Characteristics in Busan Metropolitan Area

Won Woo Choi[1,2], Eun Ji Kim[3], Soon-Hwan Lee[3,4]*

[1)]*Department of Earth Science, Pusan National University, Busan 46241, Korea*
[2)]*Busan Science High School , Busan 46235, Korea*
[3)]*Department of Earth Science Education, Pusan National University, Busan 46241, Korea*
[4)]*Institute of Environmental Studies, Pusan National University, Busan 46241, Korea*

Abstract

The purpose of this study was to analyze the cluster distribution of $PM_{2.5}$ in Busan between 2015 and 2019, focusing on spatiotemporal variability in the distribution and its causes. Based on annual and seasonal cluster analysis of $PM_{2.5}$ in Busan, in winter especially, the data was divided into two clusters, corresponding to 2015–2017 (Period 1) and 2018–2019 (Period 2). Pearson correlation coefficients were calculated and clustering was shown to be significant. In cluster analysis by period, taking measurements from each $PM_{2.5}$ observation point, a geographical shift in the clustering was observed from the east-west axis of Busan to the north-south axis. This was hypothesized to reflect interannual changes in the synoptic scale air currents in Busan. Therefore, wind speed and direction data were collected from weather monitoring stations for disaster prevention in Busan during the same period, and the ratio of the east-west and north-south components was calculated to analyze synoptic scale air currents. In both periods, the prevailing wind was along the east-west axis, but winds along the north-south axis were confirmed to become stronger from Period 1 to Period 2, and this was consistent with the changes in clustering. This analysis shows that analyzing $PM_{2.5}$ in Busan based on trends in a single period from 2015 to 2019 could lead to errors; instead, Period 1 and Period 2 should be differentiated when analyzing $PM_{2.5}$. This demonstrates the importance of investigating regional wind speed and direction for more precise analysis.

Keywords: $PM_{2.5}$, Hierarchical cluster analysis, Interannual variability

1. Introduction

Recently, many countries, including South Korea, have been suffering severe atmospheric pollution, and there has been much interest in the effects of atmospheric pollution on human health (Ko et al., 2019; Bhat et al., 2021; Zhang et al., 2022). This study focuses on particulate matter ($PM_{2.5}$), which are atmospheric pollutant with a diameter of less than 2.5 μm. $PM_{2.5}$ usually enters via the respiratory system, and due to their small size, the particles can pass through the blood vessels and cause cardiovascular or respiratory disease, or even premature death (Kim et al., 2019; Krittanawong et al., 2023). To lower $PM_{2.5}$ concentrations, the government has established a master plan and is implementing several policies to control fine dust, such as emergency measures to reduce fine dust, and a seasonal control system. As a result, the nationwide annual mean $PM_{2.5}$ concentration has shown a decreasing trend from 2015 to 2019,

Received 9 January, 2026; **Revised** 4 February 2026;
Accepted 6 February, 2026
***Corresponding author** : Soon-Hwan Lee, Department of Earth Science Education, Pusan National University, Busan 46241, Korea
Phone : +82-51-510-2706
E-mail : withshlee@pusan.ac.kr

at 26 $\mu g/m^3$, 26 $\mu g/m^3$, 25 $\mu g/m^3$, 23 $\mu g/m^3$, and 23 $\mu g/m^3$, but this is still higher than the annual average air quality standard of 15 $\mu g/m^3$ (NEIR, 2020; Son et al., 2020).

The study area, Busan, is the largest port city in South Korea and is located at the southeastern end of the Korean Peninsula. As a coastal city, Busan exhibits characteristics that are distinct from those of inland regions (Kim et al., 2020b). In particular, Busan is characterized by a highly complex geographical setting, where coastal zones, large-scale port facilities, densely populated urban areas, and surrounding mountainous terrain coexist within a relatively limited spatial extent. This heterogeneous topography facilitates frequent interactions among sea–land breezes, mountain–valley winds, marine air masses, and synoptic-scale flows, resulting in highly sensitive and spatially heterogeneous airflow structures. Such conditions can lead to pronounced local differences in atmospheric ventilation and stagnation, even under similar emission scenarios, thereby amplifying the spatial variability of $PM_{2.5}$ concentrations within the city. Spatiotemporal clustering structures of $PM_{2.5}$ are not necessarily stationary over time. For example, a study analyzing $PM_{2.5}$ distributions across 269 Chinese cities reported that spatial clustering characteristics of $PM_{2.5}$ varied between consecutive years, with the composition and boundaries of clusters reorganizing over time, highlighting the non-stationary nature of spatial clusters in air pollution fields (Zhao et al., 2019).

In addition to its coastal and topographic influences, Busan hosts the world's sixth-busiest container port, where emissions from ships, cargo handling, and port-related transportation activities are substantial. Previous studies have shown that $PM_{2.5}$ emissions from the Busan New Port can directly affect adjacent industrial areas such as Noksan-dong, depending on prevailing airflow conditions (Kang et al., 2025). Furthermore, analyses of spatial $PM_{2.5}$ distributions across western Busan, eastern Busan, and port areas have revealed particularly high concentrations in western Busan, where $PM_{2.5}$ levels are strongly correlated with road traffic emissions (Min et al., 2024). These findings indicate that Busan represents a metropolitan area in which complex terrain-driven airflow patterns and spatially heterogeneous emission sources jointly shape $PM_{2.5}$ concentration fields, making it a representative case for investigating spatiotemporal variability using cluster-based approaches.

$PM_{2.5}$ distribution patterns vary across regions due to differences in secondary aerosol formation associated with urbanization and industrial restructuring, changes in local emission sources, and long-range transport driven by synoptic meteorological conditions (Liu et al., 2020; Ying et al., 2022; Park et al., 2024; Jang et al., 2025). In addition, $PM_{2.5}$ concentrations exhibit substantial temporal variability resulting from seasonal changes, atmospheric stability, boundary layer height, and variations in meteorological fields (Yoo et al., 2022; Lee et al., 2024; Qu et al., 2025). Although numerous studies have investigated spatial patterns at regional or national scales and examined synoptic meteorological influences, relatively few studies have employed cluster-based frameworks to explicitly structure and interpret spatiotemporal interactions of $PM_{2.5}$ in cities with complex terrain and emission environments.

From a methodological perspective, previous studies have predominantly applied non-hierarchical clustering techniques, such as k-means and self-organizing maps (SOMs), to analyze $PM_{2.5}$ variability (Liu et al., 2021; Chae and Lee, 2022; Wu et al., 2023; Choi et al.,

2024). However, these approaches are limited in their ability to determine the optimal number of clusters and to interpret hierarchical relationships among clusters. Moreover, many studies rely on simple averages or representative seasonal values of spatiotemporal data, which may obscure the intrinsic multi-scale structure of $PM_{2.5}$ variability. In contrast, hierarchical clustering enables the visualization and interpretation of nested relationships among clusters through bottom-up or top-down merging processes. By capturing both synoptic- and mesoscale spatiotemporal variability, hierarchical clustering allows simultaneous comparison of structural similarities and differences among higher- and lower-order $PM_{2.5}$ groups across regions.

In South Korea, nationwide $PM_{2.5}$ monitoring began in 2015, while $PM_{2.5}$ concentration characteristics in 2020 were markedly altered by the impacts of the COVID-19 pandemic, during which reduced economic activity and human mobility led to atmospheric conditions distinct from those of previous years (Huang et al., 2024; Jiang et al., 2025). Consequently, many previous studies have focused on the five-year period from 2015 to 2019 when analyzing $PM_{2.5}$ characteristics in South Korea (Cha et al., 2020; Kim et al., 2020a; Chae and Lee, 2022; Huh et al., 2023), and the same period is adopted in this study. However, earlier studies have generally treated 2015–2019 as a single homogeneous period. Considering the phased implementation of emission reduction policies and potential changes in meteorological conditions, it is plausible that synoptic-scale airflow patterns experienced interannual variability during this period. If such interannual changes occurred, it is necessary to assess how they influenced the spatial distribution and clustering structure of $PM_{2.5}$ concentrations.

The objective of this study is to elucidate the spatiotemporal hierarchical structure of $PM_{2.5}$ concentrations in Busan during 2015–2019 and to quantitatively identify changes in clustering characteristics across different periods. By exploring the relationships among cluster evolution, meteorological factors, and regional emission sources, this study aims to analyze interannual variations in $PM_{2.5}$ concentration clusters in conjunction with synoptic-scale airflow changes. The results are expected to provide a scientific basis for developing, customized air quality management strategies tailored to the complex terrain and emission environment of coastal port cities such as Busan.

2. Materials and Methods

2.1. Data

This study used hourly measurements of $PM_{2.5}$ concentration and, as meteorological factors, hourly measurements of wind speed and direction in the Busan region. First, the hourly $PM_{2.5}$ measurements were collected from the AirKorea metropolitan air quality monitoring network. AirKorea is an open website for real-time, nationwide atmospheric pollution data managed by the Ministry of Environment, so that Korean citizens can easily and conveniently access air quality data. This website provides data on the concentration of pollutants, differentiating between the metropolitan air quality, the national background concentration, roadside air quality, suburban air quality, and port air quality networks, in order to ascertain the state of air pollution nationwide, changes and trends, and whether air quality standards are being met. For this study, the average air quality concentration measurements for the Busan City (residential) region were used. As of

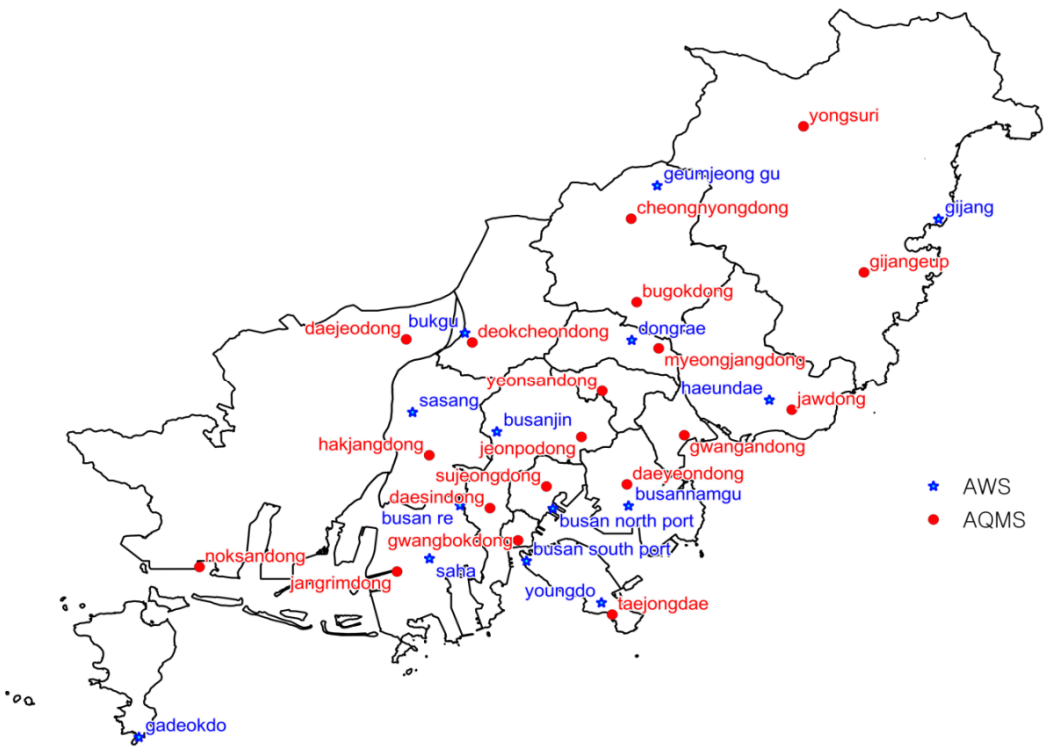

Fig 1. Spatial distribution of 19 AQMS (red circle) points that measure $PM_{2.5}$ and 14 AWS (blue star) points that automatically observe weather data located in Busan.

2025, data is being collected from 25 air quality monitoring stations (AQMS), but during the study period from January 2015 to December 2019, measurement records were available for 19 locations (Bugok-dong, Cheongryong-dong, Daejeo-dong, Daesin-dong, Daeyeon-dong, Deokcheon-dong, Gijang-eup, Gwangan-dong, Gwangbok-dong, Hakjang-dong, Jangnim-dong, Jwa-dong, Jeonpo-dong, Myeongjang-dong, Noksan-dong, Sujeong-dong, Taejongdae, Yeonsan-dong, and Yongsu-ri), and so the data from these regions was used.

Among meteorological factors, hourly wind speed and direction measurements were collected from automatic weather stations (AWS) on the Open MET Data Portal managed by the Korea Meteorological Administration. Data was collected from the 14 AWS locations in Busan: Buk-gu, Busan Namhang, Busan Weather Radar Center (Gudeok-san), Busan Bukhang, Busan Jin-gu, Busan Nam-gu, Dongnae-gu, Gadeok-do, Geumjeong-gu, Gijang-gun, Haeundae-gu, Saha-gu, Sasang-gu, and Yeongdo-gu.

Times with missing measurements for the $PM_{2.5}$ concentration were excluded from the data. Next, because rainfall causes much lower $PM_{2.5}$ measurements, times with rainfall were also excluded to minimize the confounding effects of regional characteristics. The locations of the AQMS and AWS in the Busan region are shown in Fig. 1.

2.2. Cluster analysis

Cluster analysis is a multivariate statistical method to cluster large-scale data into several groups with similar properties, and then to ascertain the characteristics of each cluster. In this study, hierarchical agglomerative clustering was used. Hierarchical cluster analysis is a technique to form a hierarchical structure by gradually merging or dividing data points to make agglomerative clusters or divisive clusters, respectively. Hierarchical cluster analysis can be applied in cases where the number of clusters is not predefined. In particular, hierarchical agglomerative clustering starts with each data point as a single cluster and gradually merges the clusters based on similarity (Govender et al., 2020). Ward's method was used to make agglomerative clusters. The Ward distance between two clusters, A and B, is defined as follows (Tuffery, 2011).

$$d(A,B) = \frac{d(a,b)^2}{n_A^{-1} + n_B^{-1}} \quad \cdots\cdots\cdots\cdots \text{Equation (1)}$$

Here, $d(A,B)$ is the Ward distance between Clusters A and B, which is calculated as the squared Euclidian distance. a and b are the centroids of their respective clusters, and n_A and n_B are the number of data points in each cluster.

The cluster analysis process in this study begins with each observation, based on the coordinates of the measurement station, starting as its own cluster. The squared Euclidian distance between all clusters is calculated, and the two clusters with the smallest distance are combined into a single cluster. The distances are then recalculated with the newly formed cluster. This process is repeated until all the observations are combined into a single cluster. This process is represented in the form of a tree-like dendrogram, and the set of clusters can be obtained for any chosen cut-off distance.

2.3. Correlation analysis

To evaluate whether the clustering process had divided the data into appropriate clusters, Pearson correlation coefficients were calculated, using hourly $PM_{2.5}$ measurements at each station. The Pearson correlation coefficients were calculated using the following equation.

$$r = \frac{\sum_{i=1}^{n}(X_i - \overline{X}) \times (Y_i - \overline{Y})}{\sqrt{\sum_{i=1}^{n}(X_i - \overline{X})^2 \sum_{i=1}^{n}(Y_i - \overline{Y})^2}} \cdots \text{Equation (2)}$$

Here, r is the Pearson correlation coefficient, X_i and Y_i are the hourly $PM_{2.5}$ measurements at two given locations in Busan, and $\overline{X}$ and $\overline{Y}$ are the mean values of the respective variables.

The Pearson correlation coefficient is a statistical index that measures the linear correlation between two variables. Correlation coefficients have a value between -1 and +1, where values close to +1 indicate a strong positive linear correlation between the two variables, values close to -1 indicate a strong negative linear correlation, and values close to 0 indicate no linear correlation.

In this study, hourly $PM_{2.5}$ measurements in 2015–2019 were used to perform Pearson correlation analysis on the AQMS, and the correlation coefficients between AQMS were compared with the AQMS cluster analysis results.

2.4. Interpolation

While $PM_{2.5}$ concentration is measured as a single point, actual $PM_{2.5}$ is distributed throughout a 3D space. Therefore, spatial

Table 1. The number of hierarchical clusters by season and year obtained from $PM_{2.5}$ data in Busan from 2015 to 2019

Year	Number of cluster			
	Season			
	Summer	Winter	Spring	Fall
2015	3	6	3	6
2016	9	6	5	6
2017	5	5	4	3
2018	4	4	5	4
2019	3	4	6	4

interpolation can be used to show the horizontal distribution, and in this study, the interpolation method was inverse distance weighting (IDW). IDW is a method of assigning weights based on the distance between unknown points and observed points, where higher weights indicate that the two points are closer together. In this way, the value of unknown points is made similar to their nearest observed neighbors. On the other hand, when two points are further apart, a lower weight will be assigned, and the observed points influence will be weaker than that of a nearer observed point (Chen and Lui, 2012). IDW interpolation is effective when the number of data points is relatively small, and is the most widely used interpolation method in these cases (Sluiter, 2009). The interpolated values of unknown points were defined as follows (Bartier and Keller, 1996; Tomczak, 1998).

$$X_{yz} = \frac{\sum_{i=1}^{n} Z_i d_{x,y,i}^{-\beta}}{\sum_{i=1}^{n} d_{x,y,i}^{-\beta}} \quad \cdots\cdots\cdots\cdots\cdots\text{Equation (3)}$$

Here, X_{yz} is the interpolated value of an unknown point, Z_i is the value of a nearby observed point, $d_{x,y,i}$ is the distance between the two points, and β is the weight.

3. Results and Discussion

3.1. Clustering of $PM_{2.5}$ concentrations in Busan by year

Based on the $PM_{2.5}$ concentrations measured in the Busan region from 2015 to 2019, in order to determine whether this period should be viewed as a single cluster or divided into several clusters, hierarchical agglomerative clustering was performed based on the longitude and latitude coordinates of each location and the $PM_{2.5}$ concentrations. The scale-adjusted distance cutoffs used in clustering were 8 for summer, 6 for winter, and 7 for spring and fall. The distance cutoff determines the number of clusters. If the cutoff value is too small the number of clusters increases. Conversely, if the cutoff value is too large, the number of clusters becomes smaller, which can result in locations with different concentration characteristics being grouped in the same cluster. The number of clusters per season and year are shown in Table 1. With the exception of spring, the number of clusters in each season can be seen to decrease over time. The number of clusters in fall and winter decreased from 6 to 4, and the number of clusters in summer decreased from 9 to 3. This is thought to be due to changes in synoptic-scale air currents due to

Table 2. Seasonal cluster types by 19 $PM_{2.5}$ concentration observation points (AQMS) in Busan are divided into A3B2, A2B3, and A2B2

AQMS number	AQMS name	Season			
		Spring	Summer	Fall	Winter
1	Gijang-eup			A3B2	A3B2
2	Yongsuri				A3B2
3	Jaw-dong				A3B2
4	Gwangan-dong		A3B2		A3B2
5	Myeongjang-dong				A3B2
6	Bugok-dong			A3B2	A3B2
7	Cheongnyong-dong				A2B3
8	Daeyeon-dong			A2B3	A2B2
9	Taejongdae			A2B3	
10	Yeonsan-dong				A3B2
11	Jeonpo-dong			A3B2	
12	Sujeong-dong			A2B3	
13	Gwangbok-dong		A3B2		A2B3
14	Daesin-dong			A2B3	
15	Deokcheon-dong				A3B2
16	Hakjang-dong				A3B2
17	Daejeo-dong			A3B2	A3B2
18	Jangrim-dong				A3B2
19	Noksan-dong		A3B2		A3B2

* A3B2: A2B3: A2B2:

climate change, and so further analysis was performed to investigate changes in wind direction. Based on the number of clusters in fall and winter, the overall study period can be broadly divided into two periods (A, B). Notably, 2018 was a year in which record-breaking cold waves and heat waves persisted from January to August, prompting the Korea Meteorological Administration to publish a special report on extreme climate events and marking a turning point at which climate change began to be recognized not as a future concern but as an immediate risk. Depending on which period 2017 is included in, these can be divided as A3B2, A2B3, or A2B2. Here, A3B2 is a split between 2015–2017 and 2018–2019, A2B3 between 2015–2016 and 2017–2019, and A2B2 between 2016–2017 and 2018–2019.

Table 2 shows the seasonal cluster distributions A3B2, A2B3, and A2B2 for $PM_{2.5}$ observation points. The blue shaded area is A3B2, the orange shaded area is A2B3, and the green shaded area is A2B2. Unshaded seasons indicate that the season showed no clear changes depending on the grouping of years.

In spring, there was no change in the seasonal clustering trends at any observation point. As shown by the blue shaded region, 12 out of the 19 AQMS demonstrated A3B2-type interannual variability in the winter clustering trends. In summer and fall as well, there were 3 and 4 AQMS, respectively, showing A3B2-type

interannual variability in seasonal clustering trends.

The orange shaded region shows that the interannual variability was A2B3-type in 4 AQMS in fall and 2 AQMS in winter, and the green shaded region shows that there was 1 A2B2-type AQMS in winter. To summarize, it can be surmised that climate change around 2017–2018 caused a change in the seasonal clustering trends for $PM_{2.5}$ concentration. In particular, 15 of the 19 AQMS showed changes in clustering trends in winter. This suggests that climate change was most prominent in winter, when it had a major impact on the distribution of $PM_{2.5}$ concentrations.

As such, the $PM_{2.5}$ clustering characteristics in winter were divided into two groups, corresponding to 2015–2017 (Period 1) and 2018–2019 (Period 2), and correlation coefficients were calculated to test whether this grouping was appropriate.

Fig. 2 shows the Pearson correlation coefficients between AQMS in Period 1 and Period 2. Lower correlation coefficients are colored blue and higher correlation coefficients are colored red. The correlation analysis results for each AQMS in winter are discussed below. First, in Fig. 2(a), the $PM_{2.5}$ correlation coefficients between AQMS in Period 1 are lower, overall, than those for Period 2 in Fig. 2(b). Second, in Period 1, Hakjang-dong (No. 16; r = 0.68–0.87), Jangnim-dong (No. 18; r = 0.55–0.75), and Noksan-dong (No. 19; r = 0.66–0.82) showed lower correlation coefficients than other AQMS during the same period, but that difference was smaller during Period 2 (Hakjang-dong, r = 0.72–0.89; Jangnim-dong, r = 0.72–0.87; Noksan-dong, r = 0.73–0.84).

These results suggest the climatic factors changed with the start of 2018, and the winter correlation analysis results suggested, like the winter cluster analysis results, that the division into Period 1 and Period 2 was significant.

The $PM_{2.5}$ clusters in Busan in winter, when divided into Period 1 and Period 2, are shown in Fig. 3. Points comprising the same cluster in each period are indicated with circles of the same color, and the correlation coefficients between the points, as tended to be high, as shown in Fig. 2. Comparing Fig. 3a and Fig. 3b shows that the distribution of $PM_{2.5}$ clusters in Busan in winter changed with the transition from Period 1 to Period 2, and the nature of these changes is discussed below. First, Cheongryong-dong, Bugok-dong, Myeongjang-dong, Yeonsan-dong, and Gwangan-dong, which are located along a valley in the north-south direction in central Busan, were combined in a single cluster. Second, Taejongdae, Sujeong-dong, Daeyeon-dong, Gwangan-dong, and Jwa-dong, located along the southern coast of Busan, were originally in the same cluster, but Taejongdae, Sujeong-dong, and Daeyeon-dong separated to form a new cluster. Third, Hakjang-dong and Jangnim-dong, lying east of the Nakdong River in west Busan, were originally in different clusters but were later joined in the same cluster. Fourth, Naksan-dong and Daejeo-dong, lying west of the Nakdong River in west Busan, were originally in different clusters but were later joined in the same cluster. The common trend across all four changes is that locations that were grouped along the east-west axis or were unrelated in Period 1 formed clusters along the north-south axis in Period 2. This variability in the clusters could have been due to changes in synoptic-scale air currents affecting the clustering trends. Therefore, wind speed and direction data from the Busan region was used to analyze interannual changes in synoptic-scale air currents.

(a) Pearson correlation coefficients in Period 1

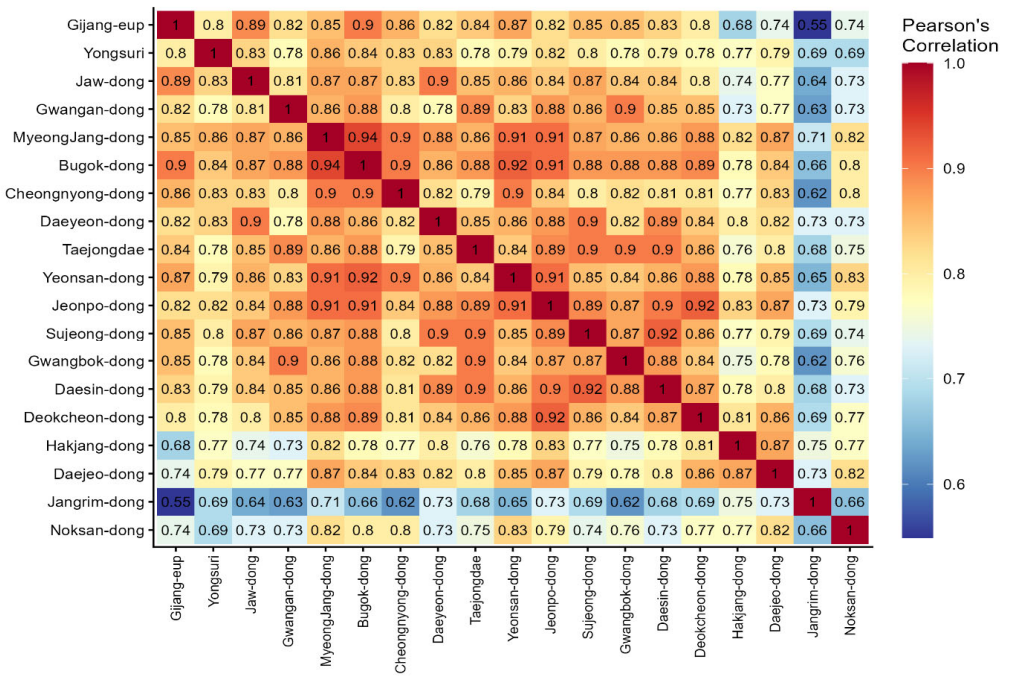

(b) Pearson correlation coefficients in Period 2

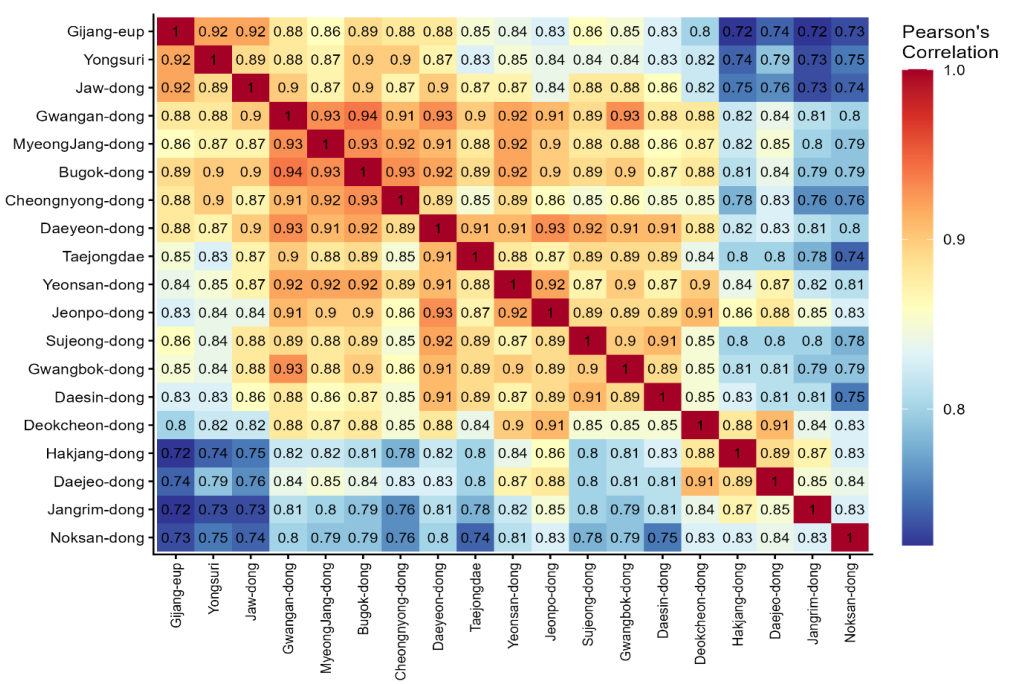

(c) Pearson coefficient difference

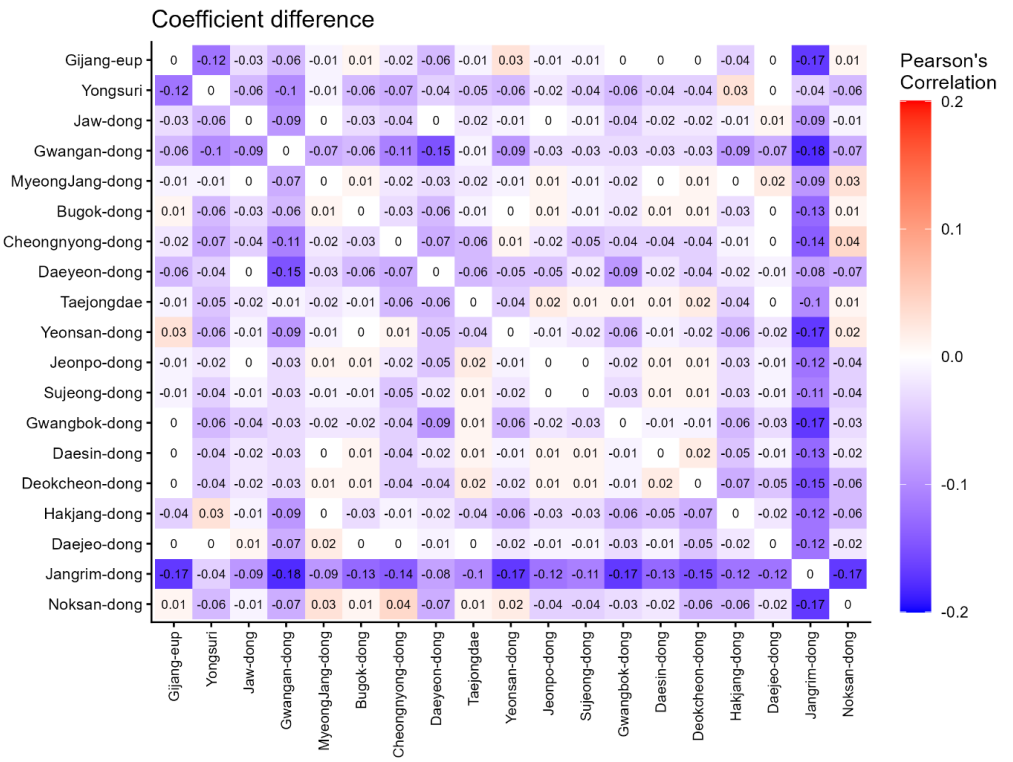

Fig. 2. Pearson correlation coefficient by Busan $PM_{2.5}$ concentration observation 19 points (AQMS) in (a) Period 1 (2015-2017), (b) Period 2 (2018-2019) and (c) Coefficient difference (Period 1 coefficient − Period 2 coefficient).

3.2. Interannual variability in overall synoptic-scale air currents in Busan

Above, the $PM_{2.5}$ concentrations confirmed that this division of the 2015–2019 study period into two groups (2015–2017, Period 1 and 2018–2019, Period 2) was significant. Next, hourly wind speed and direction measurements from AWS in Busan were used to analyze the overall synoptic-scale air currents and test for interannual variability.

Using the mean values for the east-west wind speed component (u) and the north-south wind speed component (v), the kernel density estimation (KDE) of the hourly u and v values was visualized using a joint plot, and the wind speed difference between east and west (WSD_{EW}) and wind speed difference between north and south (WSD_{NS}) at 80%, 50%, and 20% kernel densities were obtained to calculate the 'WSD_{EW}/WSD_{ND}' ratio. Here, the WSD_{EW} was calculated as umax − umin, and the WSD_{NS} was calculated as vmax - vmin. A 'WSD_{EW}/WSD_{NS}' ratio larger than 1 means that the prevailing winds were in the east-west direction, while a value close to 1 means that the east-west and north-south winds were similar, while a value lower than 1 means that the prevailing winds were in a north-south direction.

In 2015, the WSD_{EW}/WSD_{NS} ratio was 1.61 at 80% kernel density, 1.44 at 50% kernel density, and 1.47 at 20% kernel density. This means that the overall synaptic-scale air currents in Busan

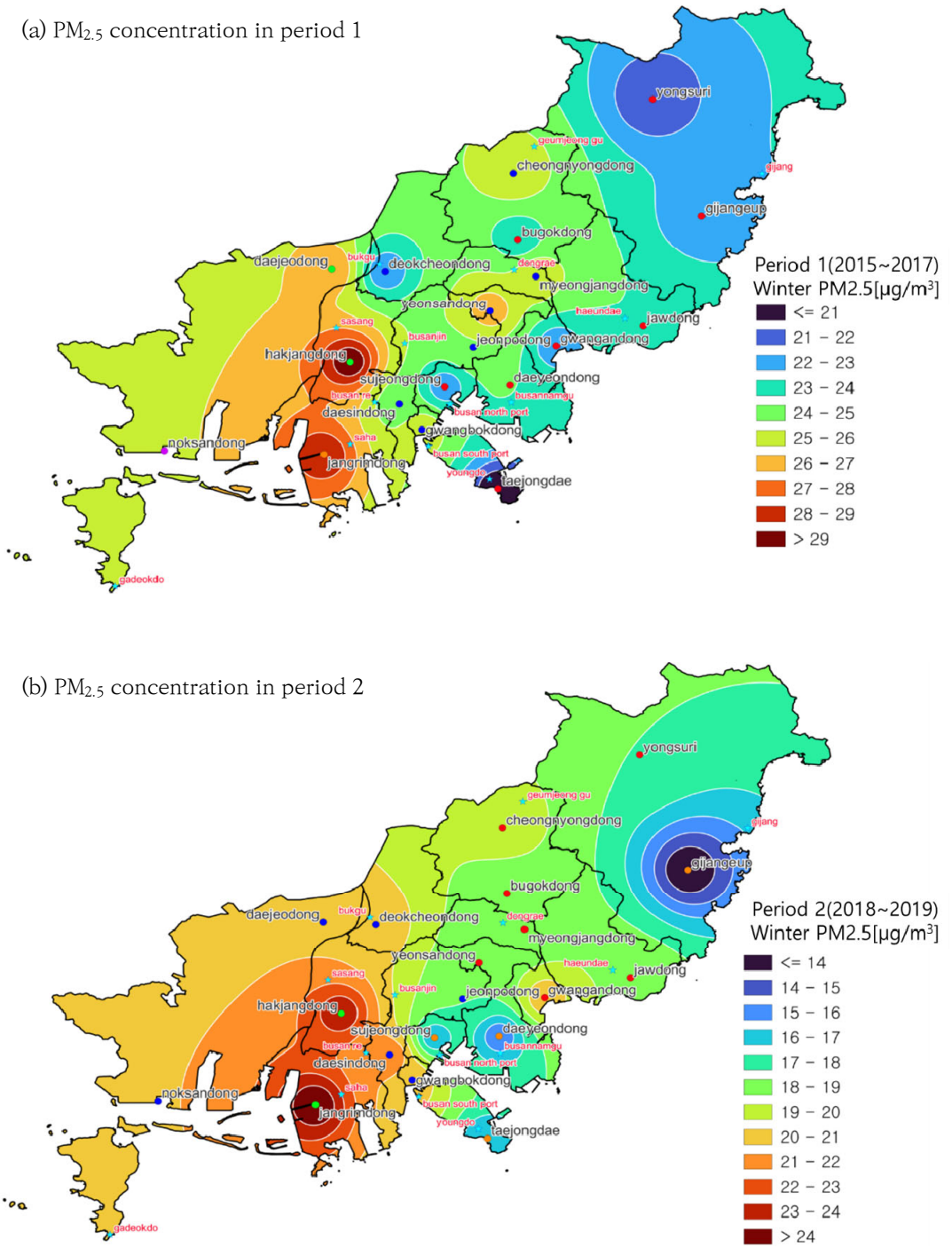

Fig. 3. Distribution of $PM_{2.5}$ concentration horizontal space in Busan by cluster by winter period (a) Period 1, (b) Period 2. Color circular symbols were classified by clustering $PM_{2.5}$ concentration observation points, and sky blue star symbols are AWS stations.

Table 3. 'WSD_{EW} / WSD_{NS}' at 80%, 50%, and 20% kernel density section for interannual analysis of synoptic-scale air currents in Busan

Year	WSD_{EW} / WSD_{NS}		
	80% kernel density	50% kernel density	20% kernel density
2015	1.61	1.44	1.47
2016	1.26	1.28	1.53
2017	1.27	1.27	1.80
2018	1.32	1.22	1.41
2019	1.29	1.10	1.35
Mean_Period 1	1.38	1.33	1.60
Mean_Period 2	1.31	1.16	1.38

in 2015 were dominated more by east-west winds than north-south winds. In 2016, compared to 2015, the WSD_{EW}/WSD_{NS} ratio decreased by 0.35 and 0.16 at 80% and 50% kernel density, respectively, showing that north-south winds were stronger relatively than in 2015. At 20% kernel density, the ratio increased by 0.06, demonstrating a slight strengthening of east-west winds. In 2017, the WSD_{EW}/WSD_{NS} ratio was 1.27 at 80% and 50% kernel density, and 1.80 at 20% kernel density. Compared to 2016, the WSD_{EW}/WSD_{NS} ratio increased and decreased by 0.01 at 80% and 50% kernel density, respectively, and increased by 0.37 at 20% kernel density, showing strengthening of east-west winds. The average WSD_{EW}/WSD_{NS} ratio in Period 1 (2015–2017) was 1.26–1.80, suggesting that overall, the prevailing winds in Busan were along the east-west axis (Table 3).

In 2018, the overall synoptic-scale air currents in Busan showed prevailing east-west winds compared to north-south winds. In 2019 as well, the east-west winds were stronger, but compared to 2018, the WSD_{EW}/WSD_{NS} ratio decreased by 0.03, 0.12, and 0.06, respectively, at 80%, 50%, and 20% kernel density, meaning that north-south winds strengthened slightly. The average WSD_{EW}/WSD_{NS} ratio in Period 2 (2018–2019) was 1.10–1.41, suggesting that overall, the prevailing winds in Busan were still along the east-west axis, like in Period 1. However, given that the WSD_{EW}/WSD_{NS} ratio in Period 1 was 1.26–1.80, Period 2 showed a decrease of 0.07, 0.17, and 0.22 in the ratio at 80%, 50%, and 20% kernel density, respectively, demonstrating that the effects of north-south winds increased compared to Period 1. In addition, the changes in the WSD_{EW}/WSD_{NS} ratio at 50% and 20% kernel density showed continually decreasing trends from 2015 to 2019. While the relatively short analysis period limits the ability to conclusively distinguish between transient variability and long-term climate-driven changes, the consistent directional shift in wind dominance provides robust evidence of non-stationary clustering behavior, indicating that the spatial boundaries between $PM_{2.5}$ concentration clusters have migrated over time rather than remaining fixed.

3.3. Interannual variability in synoptic-scale air currents per weather station

In order to investigate whether the interannual variability in overall synoptic-scale air currents in Busan could also be observed at the AWS level, after dividing the data into Periods 1 and 2, the WSD_{EW}/WSD_{NS} ratio was

calculated for each AWS, and the AWS were categorized as showing almost no interannual variability (marked as -), showing an increase in the effects of east-west winds (marked as ↑), or showing an increase in the effect of north-south winds (marked as ↓; Table 4).

Dongnae-gu and Gijang-gun both showed almost no change in interannual variability of air currents from Period 1 to Period 2 at all kernel densities. For Gudeok-san and Busan Jin-gu, apart from at 20% kernel density, Busan Nam-gu, Gudeok-san, Busan Bukhang, Busan Jin-gi, Haeundae, Saah-gu, and Sasang-gu showed strengthening of the east-west winds at most kernel densities. On the other hand, for Buk-gu, Busan Nam-gu, Gadeok-do, Geumjeong- gu, and Yeongdo-gu, the effects of east-west winds decreased at most kernel densities, and this can be interpreted as an overall increase in the influence of north-south winds in the study area.

When examining the overall interannual variability in synoptic-scale air currents per weather station, there were more stations showing strengthening of east-west winds (n=7) than those showing strengthening of north-south winds (n=5). However, the total sum of the 5 stations showing north-south wind strengthening was larger, indicating an overall strengthening of north-south winds in Busan. In addition, because Haeundae is blocked by Jang-san and Gugok-san mountains to the north, it is thought that even though synoptic-scale air currents became stronger in the north-south axis, this caused winds blowing in the east-west direction, leading to stronger east-west winds.

The interannual variability in synoptic-scale air currents at each AWS in Busan (Table 4) was analyzed with reference to Fig. 3, differentiating the horizontal distribution of $PM_{2.5}$ in winter in Periods 1 and 2 into clusters. In the transition from Period 1 to Period 2, the overall synoptic-scale air currents in Busan showed strengthening of the influence of north-south winds. This can be linked to clusters appearing along the east-west axis In Period 1, when the east-west winds were more dominant, and along the north-south axis in Period 2, when the influence of north-south winds increased. In Table 4, the interannual variability in the synoptic-scale air currents differed at each location, but was largest in Busan Nam-gu, Geumjeong-gu, Yeongdo-gu, and Haeundae. Of these, the influence of north-south winds clearly strengthened at the 3 locations other than Haeundae, and there was interannual variability in clustering. Analyzing the wind data for Haeundae-gu, even though the east-west winds became stronger, it is thought that, due to the influence of Jang-san immediately north of the weather station, the topographical effects were reflected more strongly than the interannual variation in the wind direction.

4. Conclusions

The purpose of this study was to analyze the distribution of $PM_{2.5}$ clusters in Busan over 5 years from 2015 to 2019, to investigate changes in the cluster distribution over time, and to elucidate the causes of any changes.

Using hourly $PM_{2.5}$ measurements (AQMS) from 2015–2019, hierarchical agglomerative clustering was performed by year and season, and apart from spring, all seasons showed a trend for decreasing number of clusters approaching 2019. The annual trends in the number of clusters are clearly differentiated in winter, and interannual variability was observed when dividing the study period into 2015–2017 (Period 1) and 2018–2019 (Period 2). In particular, this interannual variability was observed at 12

Table 4. Interannual variability of synoptic airflow at Busan AWS sites, classified into negligible change (–), enhanced east–west flow influence (↑), and enhanced north–south flow influence (↓). Analyses were conducted for kernel density intervals of 80%, 50%, and 20% for Periods 1 and 2

Change of $\frac{WSD_{EW}}{WSD_{NS}}$	AWS name	80% kernel density		50% kernel density		20% kernel density	
		Period 1	Period 2	Period 1	Period 2	Period 1	Period 2
$\frac{WSD_{EW}}{WSD_{NS}}$ (-)	Dongraegu	0.66	0.76	0.86	0.90	0.62	0.64
	Gijanggun	1.49	1.45	1.40	1.35	0.93	0.93
$\frac{WSD_{EW}}{WSD_{NS}}$ (↑)	Busan southport	1.12	1.16	1.39	1.85	1.59	1.75
	Gudeok mountain	2.09	2.55	1.38	1.69	1.28	1.15
	Busan northport	1.62	1.68	2.13	2.39	2.17	2.63
	Busanjingu	2.52	2.65	2.64	2.92	3.67	3.00
	Haeundaegu	0.98	1.15	0.98	1.25	1.00	1.07
	Sahagu	1.55	1.69	1.19	1.25	0.78	0.81
	Sasanggu	0.69	0.80	0.83	0.86	0.69	0.77
$\frac{WSD_{EW}}{WSD_{NS}}$ (↓)	Bukgu	1.10	0.90	0.75	0.69	0.75	0.73
	Busannamgu	1.44	1.09	1.70	1.23	1.86	1.47
	Gadeokdo	1.55	1.14	1.24	1.14	1.12	1.33
	Geumjeonggu	1.07	0.87	0.64	0.70	0.92	0.42
	Youngdogu	1.45	1.10	1.00	0.91	1.10	0.90

out of 19 $PM_{2.5}$ measurement sites. To determine whether this separation of clusters was appropriate, Pearson correlation analysis was performed using $PM_{2.5}$ measurements and geographical coordinates at each location. The correlation coefficients in Period 1 were overall lower than those in Period 2. In Period 1, Hakjang-dong, Jangnim-dong, and Naksan-dong showed lower correlation coefficients that other locations, but these increased in Period 2. In summary, like the cluster analysis results, correlation analysis also showed that clusters had different characteristics when differentiating between 2015–2017 and 2018–2019, and locations in the same cluster in a given period showed higher correlation coefficients, demonstrating that this two-period analysis was significant. In particular, locations that showed a large change in the correlation coefficient, such as Cheongryong-dong, Gwangan-dong, Hakjang-dong, and Jangnim-dong, were geographically distributed along the north-south axis. Therefore, changes in synoptic-scale air currents were surmised to have affected changes in clustering trends.

To further examine the hypothesis that interannual variability in synoptic-scale air currents was the cause of interannual variability in $PM_{2.5}$ clustering, synoptic-scale air currents were analyzed using wind speed and direction data from AWS the Busan region, and WSD_{EW}/WSD_{NS} ratios were calculated by year and location. The results of this analysis showed that, while the prevailing winds overall in Busan were along the east-west axis, the influence of north-south winds increased from Period 1 to Period 2. This is thought to be due to changes in the synoptic scale meteorological field due to climate change. When synoptic- scale air currents were analyzed at each AWS, 2 out of 14 sites showed almost no interannual variability, 7 sites showed strengthening of east-west winds,

and 5 sites showed strengthening of north-south winds. All the number of locations with east-west wind strengthening was larger, the magnitude of the interannual variability was larger for the locations with north-south wind strengthening, and so these locations had a greater impact on the interannual variability of the average synoptic- scale air currents across the whole of Busan.

In terms of the geographical distribution of $PM_{2.5}$ clusters in Busan in each period, the clusters in Period 1 tended to be formed along the east-west axis, while the same clusters in Period 2 tended to be formed along the north-south axis, which is consistent with the overall interannual variability in synoptic-scale air currents in Busan. This suggests that $PM_{2.5}$ clustering was affected near AWS locations that experienced severe interannual wind variability.

Beyond changes in the number of clusters, this study provides robust evidence that the spatial boundaries of $PM_{2.5}$ clusters in Busan are non-stationary and migrate over time in response to interannual variability in synoptic-scale circulation. The transition from east–west-oriented clustering in Period 1 to north–south-oriented clustering in Period 2 indicates that $PM_{2.5}$ clusters do not remain geographically fixed but reorganize dynamically as dominant wind regimes shift. This non-stationary clustering behavior is especially relevant in Busan, where the combined influences of coastal exposure, intensive port activity, and surrounding mountainous terrain create a meteorological environment highly sensitive to changes in airflow patterns.

Therefore, analyzing $PM_{2.5}$ in Busan as a single homogeneous period from 2015 to 2019 may lead to misinterpretation of spatiotemporal patterns. Differentiating between Period 1 and Period 2 is essential for accurately capturing interannual variability, underscoring the importance of incorporating regional wind speed and direction into $PM_{2.5}$ analyses. Under ongoing global warming and accelerating climate change, synoptic-scale circulation changes are likely to persist, making it increasingly critical to account for such variability in regional air quality assessments.

From a policy perspective, the findings of this study imply that current $PM_{2.5}$ management strategies in Busan—largely based on fixed administrative zones and source-oriented controls—may not fully reflect the dynamically shifting nature of pollution hotspots. The observed migration of cluster boundaries suggests that areas of elevated $PM_{2.5}$ concentration can change over time depending on prevailing synoptic-scale wind conditions. Incorporating spatiotemporally adaptive clustering information into air quality management frameworks could therefore enhance the effectiveness of mitigation measures, particularly in port-adjacent areas and densely populated residential zones that exhibit strong interannual variability. Such an approach would also support more flexible protection strategies for vulnerable populations, moving beyond static regional classifications.

Future research should focus on quantitatively characterizing cluster boundary mobility and linking it to specific synoptic circulation types and mesoscale meteorological processes. Integrating additional variables such as air mass trajectories, boundary layer height, and $PM_{2.5}$ chemical composition would provide deeper insight into the mechanisms driving non-stationary clustering. Extending the analysis period beyond 2019 and incorporating post-COVID-19 data will be essential for determining whether the observed boundary shifts represent transient variability or persistent structural changes under continued climate change. Furthermore, applying similar

hierarchical clustering frameworks to other coastal megacities with complex terrain would help assess the broader applicability of the non-stationary clustering behavior identified in this study.

Acknowledgments

This research was supported by the Basic Science Research Program through the National Research Foundation of Korea, funded by the Ministry of Education (RS-2020-NR049592) and Korean Government (RS-2022-NR070051). This paper is a reconstruction of the first author's master's thesis.

REFERENCES

Bartier, P. M., Keller, C. P., 1996, Multivariate interpolation to incorporate thematic surface data using inverse distance weighting (IDW), Comput. Geosci., 22(7), 795-799.

Bhat, T. H., Jiawen, G., Farzaneh, H., 2021, Air pollution health risk assessment (AP-HRA), principles and applications, Int. J. Environ. Res. Public Health, 18(4), 1935.

Cha, S. H., Han, Y. J., Bae, G. N., 2020, Spatio-temporal distribution of PM10 and PM2.5 in Gangwon province of South Korea using air pollution monitoring network data, J. Korean Soc. Atmos. Environ., 36(4), 492-506.

Chae, D. E., Lee, S. H., 2022, A Study on spatial differences in PM2.5 concentrations according to synoptic meteorological distribution, J. Environ. Sci. Int., 31(12), 999-1012.

Chen, F. W., Liu, C. W., 2012, Estimation of the spatial rainfall distribution using inverse distance weighting (IDW) in the middle of Taiwan, Paddy Water Environ., 10(3), 209-222.

Choi, W., Ho, C. H., Lee, Y., 2024, Temporal pattern classification of PM2.5 chemical compositions in Seoul, Korea using K-means clustering analysis, Sci. Total Environ., 927, 172157.

Govender, P., Sivakumar, V., 2020, Application of k-means and hierarchical clustering techniques for analysis of air pollution: A Review (1980–2019), Atmos. pollut. res., 11(1), 40-56.

Huang, J., Huang, Y., Zhang, Y., Zhang, J., 2024, Spatiotemporal evolution of PM2.5 diffusion in Cheng-Yu urban agglomeration in response to COVID-19 lockdown using complex network, arXiv preprint arXiv:2406.01502.

Huh, J. W., Youn, J. S., Park, P. M., Jeon, K. J., Park, S., 2023, Development of a prediction model for daily PM2.5 in Republic of Korea by using an artificial neutral network, Appl. Sci., 13(6), 3575.

Jang, H., Park, S. Y., Kim, Y. H., Lee, C. M. 2025, Spatiotemporal distribution characteristics of PM2.5 components in the Yeosu and Gwangyang industrial complexes, Atmos., 16(3), 241.

Jiang, Q., Wang, X., Luo, L., Yang, L., Zhang, X., Zhao, J., Xi, R., Zhao, Q., 2025, Spatial and temporal characterization of PM2.5 and meteorological factors in China during the COVID-19 period, Aerosol Air Qual. Res., 25(5), 16.

Kang, M. S., Kim, J. H., Sunwoo, Y., Hong, K. H., 2025, Analysis of fine dust impacts on Incheon and Busan port areas resulting from port emission reduction measures, Atmos., 16(5), 521.

Kim, I. J., Lee, K. Y., Lee, S. H., Kim, S. D., 2019, Characteristics and health effects of PM2.5 emissions from various sources in Gwangju, South Korea, Sci. Total Environ., 696, 133890.

Kim, D., Choi, H. E., Gal, W. M., Seo, S., 2020a, Five year trends of particulate matter concentrations in Korean regions (2015–2019): when to ventilate?, Int. J. Environ. Res. Public Health, 17(16), 5764.

Kim, J. M., Jo, Y. J., Yang, G. H., Heo, G. Y., Kim, C. H., 2020b, Analysis of recent trends of particulate matter observed in Busan - comparative study on Busan vs. Seoul metropolitan area (I), J. Environ. Sci., 29(2), 177-189.

Ko, A. R., Kim, J. W., Chang, K. H., Cha, J. W., Lee, S., M., Ha, J. C., 2019, characteristics of vertical profiles of local aerosol mass concentration according to air mass pathways over the Korean Peninsula during winter, Korean Meteor. Soc., 29(5), 525-535.

Krittanawong, C., Qadeer, Y. K., Hayes, R. B., Wang, Z., Thurston, G. D., Virani, S., Lavie, C. J., 2023, PM2.5 and cardiovascular diseases: State-of-the-Art review, Int. J. Cardiol. Cardiovasc. Risk Prev., 19, 200217.

Lee, S. J., Lee, S. H., Choi, H. J., Kim, J., Kim, M. K., 2024, Influence of local circulation on short-term variations in ground-level PM2.5 concentrations, Aerosol Air Qual. Res., 24(10), 240042.

Liu, Q., Wu, R., Zhang, W., Li, W., Wang, S., 2020, The varying driving forces of PM2.5 concentrations in Chinese cities: Insights from a geographically and temporally weighted regression model, Environ. Int., 145, 106168.

Liu, S., Gautam, A., Yang, X., Tao, J., Wang, X., Zhao, W., 2021, Analysis of improvement effect of PM2.5 and gaseous pollutants in Beijing based on self-organizing map network, Sustainable Cities Soc., 70, 102827.

Min, J. H., Kim, B. G., Ju, H., Kim, N. Y., Hwang, Y. S., Lee, S., Hong, Y. S., 2024, Analysis of the association between air pollutant distribution and mobile sources in Busan using spatial analysis, J. Environ. Health Sci., 50(3), 101-200.

NIER (National Institute of Environmental Research), 2020, Annual report of air quality in Korea, 2019, NIER-GP2020-037, Incheon, Republic of Korea.

Park, S. Y., Jang, H., Kwon, J., Cho, Y. S., Lee, J. I., Lee, C. M., 2024, Spatiotemporal distribution and source analysis of PM2.5 and its chemical components in National industrial complexes of Korea: a case study of Ansan and Siheung, Environ. Sci. Pollut. Res., 31(57), 65406-65426.

Qu, K., Wang, X., Yan, Y., Jin, X., He, L. Y., Huang, X. F., Cai, X., Shen, J., Peng, Z., Xiao, T., Vrekoussis, M., Kanakidou, M., Brasseur, G. P., Daskalakis, Nikos, Zeng, L., Zhang, Y., 2025, Unexpectedly persistent PM2.5 pollution in the Pearl River Delta, South China, in the 2015–2017 cold seasons: the dominant role of meteorological changes during the El Niño-to-La Niña transition over emission reduction, Atmos. Chem. Phys., 25(22), 16983-17007.

Sluiter, R., 2009, Interpolation methods for climate data: literature review, KNMI intern rapport 2009-04, Royal Netherlands Meteorological Institute, De Bilt, Nertherlands.

Son, K. W., Kim, E. H., Bae, M. A., You, S. H., Kang, Y. H., Kim, H. C., Kim, B. U., Kim, S. T., 2020, Evaluations on PM2.5 concentrations and the population exposure levels for local authorities in South Korea during 2015-2017, J. Korean Soc. Atmos. Environ., 36(6), 806-819.

Tomczak, M., 1998, Spatial interpolation and its uncertainty using automated anisotropic inverse distance weighting (IDW)-cross-validation/jackknife approach, Environ. Sci., 2(2), 18-30.

Tufféry, S., 2011, Data mining and statistics for decision making. John Wiley & Sons, Hoboken, New Jersey, USA.

Wu, X., Wen, Q., Zhu, J., 2023, An Ensemble model for PM2.5 concentration prediction based on feature selection and two-layer clustering algorithm, Atmos., 14(10), 1482.

Ying, N., Duan, W., Zhao, Z., Fan, J. 2022, Complex networks analysis of PM2.5: transport and clustering, Earth Syst. Dyn. Discuss., 2022, 1-18.

Yoo, J. W., Park, S. Y., Lee, K., Lee, D., Lee, Y., Lee, S. H., 2022, Impacts of plateau-induced lee troughs on regional PM2.5 over the Korean Peninsula, Atmos. Pollut. Res., 13(7), 101459.

Zhang, L., Li, X., Chen, H., Wu, Z., Hu, M., Yao, M., 2022, Haze air pollution health impacts of breath-borne VOCs, Environ. Sci. Technol., 56, 12, 8541-8551.

Zhao, X., Zhou, W., Han, L., Locke, D., 2019, Spatiotemporal variation in PM2.5 concentrations and their relationship with socioeconomic factors in China's major cities, Environ. Int., 133, 105145.

• Researcher. Won Woo Choi
Department of Earth Science, Pusan National University
dnjsdn95@naver.com
• Ph.D. Eun Ji Kim
Department of Earth Science Education, Pusan National University
eunji1024@pusan.ac.kr
• Professor. Soon-Hwan Lee
Department of Earth Science Education, Pusan National University
withshlee@pusan.ac.kr